Experimental $A\ ^2\Pi$ potentials for Li-He and Li-Ne molecules

L. C. Balling and J. J. Wright
Physics Department, University of New Hampshire, Durham, New Hampshire 03824

Mark D. Havey
Physics Department, Old Dominion University, Norfolk, Virginia 23508

(Received 9 February 1982)

The well depths of the $A\ ^2\Pi$ potentials for Li-He and Li-Ne molecules have been determined by the observation of the intensity of the red wing of the Li D lines, perturbed by He and Ne, as a function of temperature and with the use of the quasistatic theory of line broadening. Significant enhancement of the fluorescence signal was achieved by the use of cw dye-laser excitation and by the operation of the fluorescence cell at low temperatures. For Li-He, we obtained $D_e = 850(100)\ \text{cm}^{-1}$; for Li-Ne, we obtained $D_e = 225(30)\ \text{cm}^{-1}$.

I. INTRODUCTION

Recently we reported measurements[1,2] of the temperature dependence of the red wing of the Na D lines perturbed by He and Ne. From these measurements, $A\ ^2\Pi$-state potentials for the Na-Ne and Na-He molecules were generated, using the quasistatic theory of line broadening employed in the pioneering experiments of Gallagher and coworkers.[3–6] In our experiment, the wing fluorescence signals were significantly enhanced by the use of a cw dye laser to excite the Na atoms and by the use of a technique borrowed from optical-pumping experiments[7] which permitted operation of the fluorescence cell at temperatures as low as 130 K.

The present work is an extension of these experiments to the study of Li-He and Li-Ne molecules. Although the experimental method was essentially the same, the low vapor pressure and the reactive properties of Li metal made the performance of these experiments considerably more difficult. We report here our observations of the red-wing intensity of the Li D lines, perturbed by He and Ne, as a function of temperature, and present experimental $A\ ^2\Pi$ potentials for the Li-He and Li-Ne van der Waals molecules. The well depths of the potentials are determined directly from the experimental data, but the shape of the $A\ ^2\Pi$ potential and, in particular, the equilibrium separation cannot be determined from the data without the use of an assumed ground-state potential. We present $A\ ^2\Pi$ potentials as a function of internuclear distance, based on appropriate $X^2\Sigma^+$ potentials, and we also present our experimental data in a form which allows one to generate $A\ ^2\Pi$ potentials from any other $X\ ^2\Sigma^+$ potential one chooses.

II. EXPERIMENT

In this experiment Li vapor was maintained in a fluorescence cell containing a helium or neon buffer gas, and the temperature of the cell was varied while keeping the Li density essentially constant. The Li atoms were excited to the $2p\ ^2P_{1/2,3/2}$ states by a cw dye laser tuned to 6708 Å, and the fluorescence intensities of the resonance line and of the buffer-gas induced red wing were measured as a function of wavelength and cell temperature.

A block diagram of the apparatus and the fluorescence cell is shown in Fig. 1. The setup is

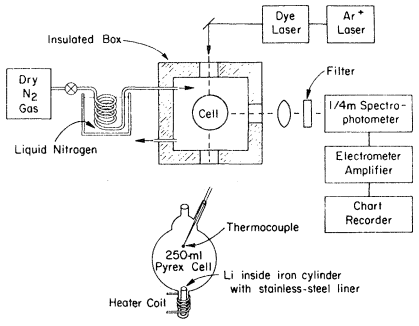

FIG. 1. A block diagram of the apparatus and the fluorescence cell. Li vapor diffused up from a heated sidearm, and the main cell volume was cooled with a flow of cold N_2 gas.

similar to that described in Ref. 1. The dye laser was pumped by an argon-ion laser and its output power was typically 0.5 W within a bandwidth of 0.5 cm^{-1}. The fluorescence was observed with a $\frac{1}{4}$-m spectrophotometer with a bandwidth of 40 Å. Before entering the spectrometer the fluorescence passed through a filter which reduced the resonance-line intensity relative to the wing fluorescence by a factor of 10.

The fluorescence cell was permanently attached to a vacuum-gas-handling system to facilitate changes of buffer gas and of buffer-gas pressure. The cell was located in an insulated enclosure, the temperature of which was varied over the range 130–375 K. Cooling of the enclosure and cell was accomplished by a flow of N_2 gas cooled by liquid nitrogen. The enclosure windows were evacuated Pyrex cylinders with the outer faces heated to prevent frosting.

For Li, the design of the cell was not as straightforward as was the case for Na, although the principle of operation was the same. The lithium density was maintained in the 250-cm^3 Pyrex cell by the diffusion and convective transport of vapor emanating from a 10-mm-diameter tubulation attached to the bottom of the cell. This tubulation contained a quantity of lithium metal which was heated by a small oven surrounding the tubulation and insulated from the enclosure.

Because of the low thermal conductivity of the cell walls and the large ratio of cell surface area to the cross-sectional area of the tubulation, the temperature of the enclosure determined the temperature in the interior of the cell. The cell temperature and the density of lithium atoms were controlled independently.

In the case of Na, the metal was simply distilled into the Pyrex tubulation, but this was not possible for Li since hot Li cracks Pyrex and quartz. The Li metal was contained in an iron cylinder, with one end open, which was inserted into the tubulation. Because it was necessary to outgas the Li reservoir at temperatures in excess of 600 °C, the tubulation was quartz instead of Pyrex. At high buffer-gas pressures, it is difficult to achieve the required Li density in the cell, and it was necessary to equip the iron cylinder with an interior stainless-steel sleeve, which was wet by the molten Li, so that the molten metal crept right up to the rim of the iron cylinder. The entire cylinder could not be constructed of stainless steel because in this case the molten Li would creep over the rim and down the outside cylinder wall, where it would come in contact with the quartz.

The temperature in the interior of the fluorescence cell was measured with a thermocouple located inside the cell near the interaction region.

III. RESULTS

Figures 2 and 3 show the observed variation of the red-wing fluorescence intensity as a function of cell temperature at various wavelengths for He and Ne buffer gases. The results shown are for constant excited-state Li density and constant buffer-gas density, and they correspond to what one expects on the basis of the quasistatic theory of line broadening in the limit of high buffer-gas density.

In the high-pressure limit, the populations of the bound and unbound excited states of the alkali–rare-gas system are in thermal equilibrium, and the wing intensity I_λ relative to the total integrated fluorescence I_0 in an optically thin sample is

$$I_\lambda / I_0 \propto n_0 e^{-[V_e(R)-V_e(\infty)]/kT}, \tag{1}$$

where n_0 is the buffer-gas density, T is the cell temperature, R is the alkali–rare-gas internuclear separation corresponding to an emission wavelength λ, and V_e is the $A\,^2\Pi$ potential. $V_e(\infty)$ is the energy of the Li $2p\,^2P_{1/2,3/2}$ state.

In the high-pressure limit one expects plots of $\ln(I_\lambda/I_0)$ as a function of $1/kT$ to yield straight lines, the slopes of which are independent of buffer-gas density. Furthermore, I_λ/I_0 at fixed temperature should increase linearly with buffer-gas density. Measurements were made over a wide

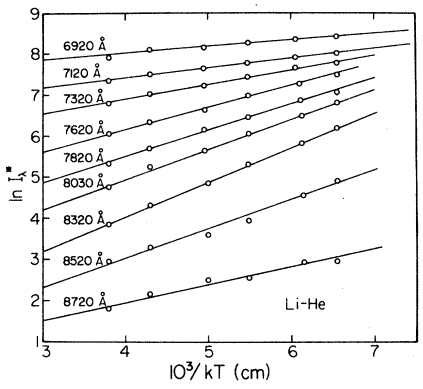

FIG. 2. Typical semilogarithmic plots of I_λ/I_0 as a function of $1/kT$ for Li-He at various emission wavelengths. For plotting convenience, we have graphed $\ln I_\lambda^*$ vs $1000/kT$, where $\ln I_\lambda^* = \ln(I_\lambda/I_0) + \text{arbitrary}$ constant. Data were obtained with a He buffer-gas pressure of 1400 Torr.

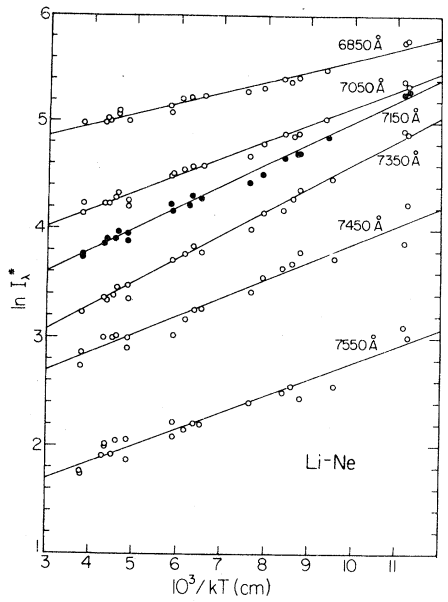

FIG. 3. Typical semilogarithmic plots of I_λ/I_0 as a function of $1/kT$ for Li-Ne at various emission wavelengths. For plotting convenience, we have graphed $\ln I_\lambda^*$ vs $1000/kT$, where $I_\lambda^* = \ln(I_\lambda/I_0) + \text{arbitrary constant}$. Data were obtained with a Ne buffer-gas pressure of 700 Torr.

range of buffer-gas densities corresponding to room-temperature pressures of 550–1450 Torr for He and 250–850 Torr for Ne, and the data conformed to what one expects in the high-pressure limit. We operated at the lowest possible Li density, and an order-of-magnitude increase of the Li density produced no change in the results, indicating that the sample was optically thin.

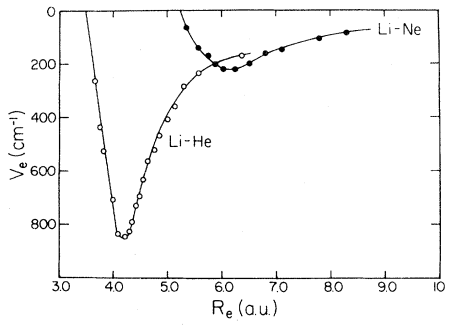

FIG. 4. $A\,^2\Pi$-state potentials for Li-He and Li-Ne generated from our experimental data and an assumed $X\,^2\Sigma^+$-state potential corresponding to the semiempirical calculation of Pascale and Vandeplanque (Ref. 8).

TABLE I. Our experimental values of V_e of V_g corresponding to various red-wing fluorescence wavelengths for Li-Ne. This data give V_e as a function of V_g and can be used to check any given set of theoretical calculations of $V_e(R)$ and $V_g(R)$.

Wavelength (Å)	$V_e(\infty)-V_e$ (cm^{-1})	V_g (cm^{-1})
6800	85	115
6850	105	205
6950	145	375
7050	160	565
7150	200	725
7250	220	900
7350	220	1080
7400	200	1195
7450	170	1320
7550	140	1510
7650	65	1775

In accordance with the Frank-Condon principle, the emission wavelength λ is given by

$$\frac{hc}{\lambda} = V_e(R) - V_g(R)\,, \tag{2}$$

where $V_g(R)$ is the $X\,^2\Sigma^+$ potential. Slopes obtained from plots such as those shown in Figs. 2 and 3 give $V_e(R)$ and $V_g(R)$ for an observed emis-

TABLE II. Our experimental values for V_e and V_g corresponding to various red-wing fluorescence wavelengths for Li-He. This data can be used to check any given set of theoretical calculations of $V_e(R)$ and $V_g(R)$.

Wavelength (Å)	$V_e(\infty)-V_e$ (cm^{-1})	V_g (cm^{-1})
6920	170	285
7120	235	625
7220	285	775
7320	255	895
7420	400	1030
7520	470	1140
7620	520	1265
7720	560	1395
7820	630	1490
7920	690	1590
8020	730	1710
8120	785	1805
8220	825	1920
8320	845	2045
8420	835	2200
8520	700	2470
8620	525	2780
8720	435	3000
8820	260	3310

TABLE III. A comparison of our experimental results with theoretical values for the well depth D_e and equilibrium separation R_e for the $A\ ^2\Pi$ potential of Li-He. The value of R_e listed in the experimental column is obtained by combining our results with a given theoretician's calculated $X\ ^2\Sigma^+$ potential.

Reference	D_e (cm^{-1}) theory	R_e (a.u.) theory	D_e (cm^{-1}) this expt.	R_e (a.u.) this expt. and theory
8	18	6.75	850	4.15
9			850	3.88
10	500	3.7	850	4.25
11	500	3.5	850	3.95
12,13	1250	3.0	850	3.60
14			850	4.5
15	850	3.5	850	4.4

sion wavelength λ, corresponding to some value of R. If one assumes the validity of a particular theoretical potential $V_g(R)$, the data immediately give V_e as a function of R.

For Li-He, numerous calculations of the $X\ ^2\Sigma^+$-state potential have been made,[8–15] and the potential calculated by Pascale and Vandeplanque,[8] which was normalized to experimental scattering data, falls in the middle of the spread of results; therefore we chose Pascale and Vandeplanque's $X\ ^2\Sigma^+$-state potentials to generate $A\ ^2\Pi$ state potentials from our data, and these potential curves are shown in Fig. 4. These curves are presented by way of illustration only, as the use of other calculated ground-state potentials alters the shape of the $A\ ^2\Pi$-state well and shifts the position of its minimum. The well depth D_e, however, is fixed by the maximum slope obtained from plots of the type shown in Figs. 2 and 3 and thus is determined unambiguously by this experiment.

For the $A\ ^2\Pi$-state of Li-He, we found

$$D_e = 850(100)\ cm^{-1}\ .$$

For the $A\ ^2\Pi$-state of Li-Ne,

$$D_e = 225(30)\ cm^{-1}\ .$$

In order that our experiment data can be used to check future theoretical calculations of the $A\ ^2\Pi$-state and $X\ ^2\Sigma^+$-state potentials, we have presented tables of our experimental values for V_e and V_g corresponding to various emission wavelengths. The tables essentially give V_e as a function of V_g, and can be immediately compared with any given set of theoretical calculations of $V_e(R)$ and $V_g(R)$. Table I is for Li-Ne; Table II is for Li-He.

In Tables III and IV we compare our experimental results with the numerous calculations of Li-He and Li-Ne potentials in the literature. In each case we compare our results with a matched pair of ground-state and excited-state potentials calculated by the same theoreticians. Using a particular theoretician's calculated $X\ ^2\Sigma^+$ potential, we generate from our data an $A\ ^2\Pi$ potential characterized by an equilibrium separation R_e. We then compare this and our experimental value for D_e with the theoretician's own values for R_e and D_e.

IV. CONCLUSION

The results of this experiment and of our earlier experiments on Na show that the $A\ ^2\Pi$ states of Li-

TABLE IV. A comparison of our experimental results with theoretical values for the well depth D_e and equilibrium separation R_e for the $A\ ^2\Pi$ potential of Li-Ne. The value of R_e listed in the experimental column is obtained by combining our results with a given theoretician's calculated $X\ ^2\Sigma^+$ potential.

Reference	D_e (cm^{-1}) theory	R_e (a.u.) theory	D_e (cm^{-1}) this expt.	R_e (a.u.) this expt. and theory
8	17	8.0	225	6.1
15	289	4.5	225	5.0

Ne and Na-Ne are definitely bound and that the $A\,^2\Pi$ binding energies for Na-He and Li-He are comparable to those for the heavier alkali—rare-gas systems.

ACKNOWLEDGMENT

This work was supported by the National Science Foundation and the Air Force Office of Scientific Research.

[1]M. D. Havey, S. E. Frolking, and J. J. Wright, Phys. Rev. Lett. 45, 1783 (1980).
[2]M. D. Havey, S. E. Frolking, J. J. Wright, and L. C. Balling, Phys. Rev. A 24, 3105 (1981).
[3]R. E. M. Hedges, D. L. Drummond, and A. Gallagher, Phys. Rev. A 6, 1519 (1972).
[4]C. Carrington and A. Gallagher, J. Chem. Phys. 60, 3436 (1974).
[5]G. York, R. Scheps, and A. Gallagher, J. Chem. Phys. 63, 1052 (1975).
[6]R. Scheps, C. Ottinger, G. York, and A. Gallagher, J. Chem. Phys. 63, 258 (1975).
[7]J. J. Wright, L. C. Balling, and R. H. Lambert, Phys. Rev. A 1, 1018 (1970).
[8]J. Pascale and J. Vandeplanque, J. Chem. Phys. 60, 2278 (1974).
[9]Nivard Scheel and Virginia Griffing, J. Chem. Phys. 36, 1453 (1962).
[10]S. B. Schneiderman and H. H. Michels, J. Chem. Phys. 42, 3706 (1965).
[11]M. Kraus, P. Maldonado, and Arnold C. Wahl, J. Chem. Phys. 54, 4944 (1971).
[12]C. Bottcher, A. Dalgarno, and E. L. Wright, Phys. Rev. A 5, 1606 (1973).
[13]C. Bottcher, T. C. Cravens, and A. Dalgarno, Proc. R. Soc. London, Ser. A 346, 157 (1975).
[14]Patricia Dehmer and Lennard Wharton, J. Chem. Phys. 57, 4821 (1972).
[15]Graeme Roberts, private communication.